THE JOURNAL OF PHYSICAL CHEMISTRY B

ARTICLE

pubs.acs.org/JPCB

Positioning of Antioxidant Quercetin and Its Metabolites in Lipid Bilayer Membranes: Implication for Their Lipid-Peroxidation Inhibition

Pavlína Košinová,[†,‡] Karel Berka,[‡] Michael Wykes,[§] Michal Otyepka,[‡] and Patrick Trouillas*[,†,§]

[†]LCSN−EA1069, School of Pharmacy, Université de Limoges, 2 rue du Dr. Marcland, 87025 Limoges, France

[‡]Regional Center of Advanced Technologies and Materials, Department of Physical Chemistry, Faculty of Science, Palacký University, 17. listopadu 1192/12, 77146 Olomouc, Czech Republic

[§]Laboratoire de Chimie des Matériaux Nouveaux, Université de Mons, Place du Parc 20, 7000 Mons, Belgium

Supporting Information

ABSTRACT: Among numerous biological activities, natural polyphenols are antioxidants widely distributed in plants capable of inhibiting lipid peroxidation, which belongs to the most serious degenerative cell processes. Positioning of antioxidants in lipid bilayers can provide an insight to the lipid-peroxidation inhibition at the molecular level. This work aims at determining the location and orientation of quercetin and its most representative (glucuronidated, methylated, and sulfated) metabolites in lipid bilayer via molecular dynamic simulations. We show that quercetin derivatives penetrate the lipid bilayer and that the depths of penetration depend on molecular charge and substitutional variations. In the presence of charged substituents (sulfates and glucuronidates), the molecule is pulled toward the lipid bilayer surface. The orientation also depends on substitution as H-bonds are formed between the polar head groups of the bilayer and the (i) OH groups, (ii) sugar, and (iii) sulfate moieties of the antioxidants. As flavonoids and their derivatives are preferentially localized in the lipid bilayer membrane or on the bilayer/water interface, they readily concentrate in a relatively narrow membrane region. Despite the low concentrations of flavonoids in food, their spatial confinement in the membrane greatly enhances their local concentration in this vital region, thus increasing their importance for in vivo biological activities including oxidative stress defense.

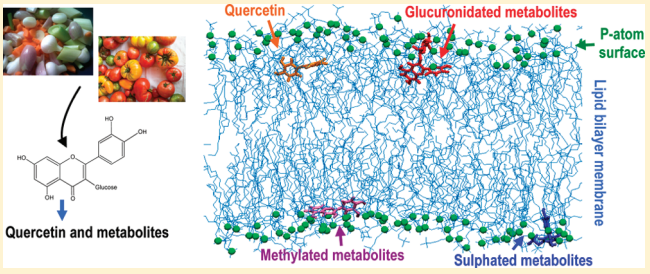

1. INTRODUCTION

Biological membranes are viscous liquids playing an important role in cell life constituting a selective barrier between intra- and extracellular environments. They are composed of different types of lipids (phospholipids, glycolipids, cholesterol), proteins, and other organic molecules (e.g., vitamin E) affecting membrane features (e.g., fluidity and thickness).[1−3] Among the numerous biological processes occurring in the vicinity of membranes, oxidative stress (due to, e.g., pollution, X-ray, UV-light) continuously attacks the lipid bilayer, which induces lipid peroxidation. The subsequent production of reactive oxygen species (ROS)[4−6] is partially responsible for degenerative processes in cells, which may initiate various diseases and aging.[7] In order to counteract these deleterious effects, endogenous and exogenous antioxidants may act as free radical scavengers in membranes to prevent, slow down, or even stop this oxidative process.[8−10]

Polyphenols are a wide class of natural secondary plant metabolites. They are widely distributed in plants and are part of the human diet (e.g., fruit, vegetables, spices, beverages made from plants including tea, chocolate, wine, fruit juices, herbal tea, and beers). They are divided into many subgroups (including simple phenols, phenolic acids, flavonoids, lignans, flavonolignans, depsides, tannins) according to their chemical structures, and have been widely studied for their protective activities against cardiovascular diseases, cancer, aging, and degenerative pathologies.[11] Among their many other biological activities, they are powerful antioxidants. The presence of phenolic OH groups and π-electron conjugation favor HAT to free radicals, which are scavenged and inactivated.[12] Free-radical scavenging by polyphenols is correlated to their capacity to inhibit lipid peroxidation.[13] However, like other biological activities, the inhibition of lipid peroxidation should also be related to the capacity of these compounds to interact with and penetrate lipid bilayers. This mainly depends on polyphenol lipophilicity. This parameter can be estimated by the partition coefficient, log *P*, defined for a given molecule as the ratio of concentrations in the two phases of a mixture of immiscible solvents (e.g., water and octanol) at equilibrium; the higher the log *P*, the higher the lipophilicity. Nonetheless, log *P* empirically estimates the global lipophilicity of the compound and does not give the exact location (or depth

Received: September 9, 2011
Revised: December 2, 2011
Published: December 27, 2011

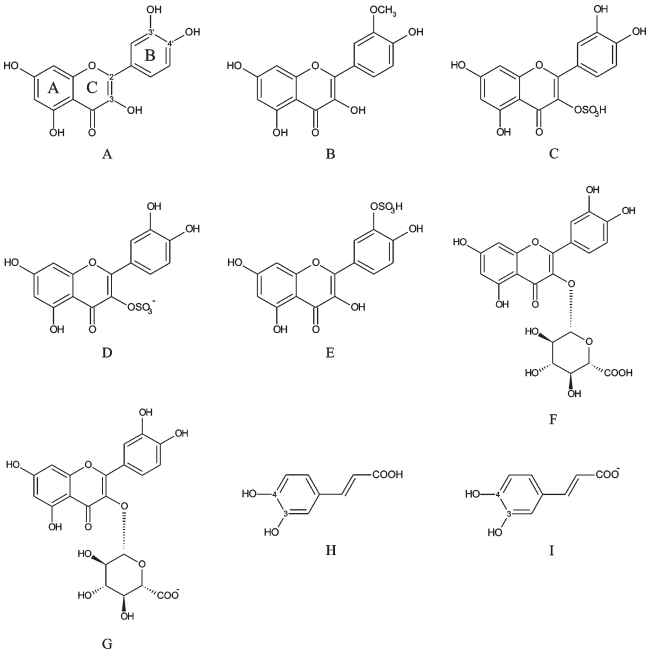

Figure 1. Molecular structures of (A) quercetin, (B) 3′-*O*-methylquercetin, (C) protonated form of quercetin-3-*O*-sulfate, (D) quercetin-3-*O*-sulfate, (E) protonated form of quercetin-3′-*O*-sulfate, (F) protonated form of quercetin-3-*O*-glucuronide, (G) quercetin-3-*O*-glucuronide, and (H) protonated and (I) nonprotonated caffeic acid.

penetration) and orientation of the compounds in lipid membranes. Polyphenols are amphipathic molecules, aromatic rings and the hydroxyl groups being hydrophobic and hydrophilic, respectively. The location and orientation of polyphenols in membranes depend on the number and positions of OH groups.[14−16]

The location of natural polyphenols, e.g., flavonoids, in membranes remains controversial. Some experimental studies suggest that flavonoids with numerous polar OH groups (e.g., quercetin and catechin) are located deep inside membranes.[13,17] Other studies locate flavonoids closer to the membrane surface where they can interact with the polar head-groups of lipids via H-bonding.[18−20] The location and orientation of flavonoids affect membrane structure and function, notably their fluidity,[16,21−23] ability to conduct ions,[17] and volume.[24] The location of flavonoids inside membranes depends strongly on pH and flavonoid charge;[17] the lower the pH, the lower the deprotonation state and the deeper the penetration. The antioxidant quercetin is one of the most studied flavonoids since it possesses several chemical characteristics that make this molecule a free-radical scavenger of reference, the 3′-OH, 4′-OH, and 3-OH groups (Figure 1) being the most active groups.[12,25] It is found as glycoside in high concentrations in many types of fruit and vegetables. Nonetheless, quercetin itself rarely exists unmodified in the living organism. It is usually transformed in the liver during the phase II of metabolism of xenobiotics; i.e., conjugation reactions to form methylated, sulfated, and glucuronidated derivatives.[26−28] The most representative quercetin conjugates (Figure 1) are (i) 3′-*O*-methyl-quercetin, (ii) quercetin-3-*O*-sulfate, (iii) quercetin-3′-*O*-sulfate, and (iv) quercetin-3-*O*-glucuronide.[26,28,29] Another studied representative of polyphenolic compounds is caffeic acid which is together with its derivatives widely distributed in plants and is a powerful antioxidant. It also reflects the behavior of small metabolites formed after ingestion of flavonoid compounds. The metabolism process usually increases hydrophilicity, solubility, transport, and subsequently bioavailability. The capacity of the metabolites to incorporate into the membrane and inhibit lipid peroxidation maybe modified compared to quercetin itself. This work aims at rationalizing the position and orientation of quercetin and quercetin metabolites (Figure 1) in a model membrane by molecular dynamics (MD). This methodology is validated and discussed (section 3.1) on the basis of data available in the literature concerning the interaction of quercetin with membranes. The influence of conjugation that occurs during the phase II metabolism pathway is then discussed in section 3.2. The correlation between the location/orientation of the different compounds and their ability to act as antioxidant (e.g., lipid peroxidation inhibitor) is thus rationalized according to MD simulations (sections 3 and 4).

2. METHODS

2.1. Bilayer Membrane Model. The lipid bilayer model comprises 128 1,2-dioleoyl-*sn*-glycero-3-phosphatidylcholine (DOPC) molecules surrounded by at least 3810 molecules of water. Phosphatidylcholines are the dominant lipid species in many membranes, including cell membranes or membranes of the endoplasmic reticulum.[3] The oleoyl chain of DOPC contains a double bond between C9 and C10 (see Table 1 for numbering). The Berger force field was used to model DOPC,[30] as this force field is known to reproduce coarse properties of DOPC lipid bilayer rather well.[31] Explicit water molecules were described by the SPC (single point charge) model.[32] Before any calculation in the presence of the antioxidant, the lipid bilayer model was pre-equilibrated by 100 ns MD simulations.

The most stable conformations of quercetin and metabolites were optimized at the DFT B3P86/6-31+G(d,p) level, well adapted for polyphenols,[12] prior to generation of restrained fit of electrostatic potential (RESP)[33] and PRODRG[34] partial atomic charges for use in conjunction with the Gromos 53a6 force field.[35] The parametrization methodology implemented in the PRODRG 2.5 program is widely used in MD simulations of drugs;[36] however, the applicability of PRODRG charges for molecular simulations has been questioned in the literature, because PRODRG charges do not reproduce well partitioning between nonpolar and polar phases.[37] The partial charges are crucial in particular for a reasonably accurate description of noncovalent interactions due to the long-range nature of electrostatic interactions.[38] The PRODRG underestimates charges of OH groups compared to RESP.[37] RESP charges are known to perform reasonably well for a wide set of molecular systems.[38] Gas-phase RESP HF/6-31G* are often used in the simulation of biomolecules in aqueous solution as this level of theory overestimates the true gas-phase dipole moment by 10−20%, thus implicitly damping the lack of condensed-phase polarization present in additive force fields using charges calculated in the gas phase. Given that the dielectric environments of the lipid and water phases are quite different, it is questionable how accurately relative free energies can be computed using a single fixed charge distribution for both phases. The description of solute charge distribution being particularly important in this study, we thus chose to perform calculations using two sets of partial charges (PRODRG and B3P86/6-31+G(d,p) RESP) with lower and higher dipole moments, respectively, thus representing cases of weak or strong polarization. Quercetin dipole moments were 3.3 and 5.6 D respectively, in comparison to the HF/6-31G* RESP

Table 1. Average Distances *d* (nm) from the Center of Lipid Bilayer and Standard Deviations Calculated for (A) Various Groups of Quercetin (See Numbering in Figure *1*) and Its Conjugates and Caffeic Acid and (B) the C- and O-Atoms of DOPC

A)

	3OH	4O	5OH	7OH	3'OH	4'OH	SO_3	COOH	COM
Quercetin	1.4 ± 0.2	1.5 ± 0.2	1.5 ± 0.2	1.5 ± 0.2	1.5 ± 0.2	1.4 ± 0.2	-	-	1.5 ± 0.2
3'-O-methyl-quercetin	1.9 ± 0.2	1.9 ± 0.2	1.9 ± 0.2	1.6 ± 0.2	1.7 ± 0.2	1.7 ± 0.2	-	-	1.8 ± 0.2
Quercetin-3-O-sulfate *	-	1.3 ± 0.3	1.3 ± 0.3	1.3 ± 0.2	1.5 ± 0.2	1.5 ± 0.1	1.4 ± 0.2	-	1.4 ± 0.2
Quercetin-3-O-sulfate	-	2.0 ± 0.1	2.0 ± 0.1	1.7 ± 0.1	2.0 ± 0.5	2.1 ± 0.4	2.3 ± 0.2	-	2.1 ± 0.2
Quercetin-3'-O-sulfate *	1.6 ±0.2	1.4 ± 0.2	1.2 ± 0.2	1.2 ± 0.2	-	2.0 ± 0.2	1.8 ± 0.2	-	1.6 ± 0.2
Quercetin-3'-O-sulfate	1.9 ± 0.2	1.8 ± 0.2	1.6 ± 0.2	1.5 ± 0.2	-	2.0 ± 0.3	2.2 ± 0.1	-	1.9 ± 0.1
Quercetin-3-O-glucuronide *	-	1.6 ± 0.1	1.5 ± 0.1	1.4 ± 0.1	1.5 ± 0.3	1.3 ± 0.3	-	1.1 ± 0.1	1.4 ± 0.1
Quercetin 3-O-glucuronide	-	1.8 ± 0.2	1.6 ± 0.2	1.2 ± 0.2	1.8 ± 0.3	1.7 ± 0.3	-	2.2 ± 0.1	1.8 ± 0.2
Caffeic acid *	1.5 ± 0.2	1.5 ± 0.2	-	-	-	-	-	0.9 ± 0.2	1.2 ± 0.1
Caffeic acid	2.2 ± 0.2	2.0 ± 0.2	-	-	-	-	-	2.6 ± 0.2	2.3 ± 0.1

* Protonated forms of derivatives are not present in physiological conditions.

B)

Atom	O	C_1	C_2	C_3	C_4	C_5	C_6	C_7	C_8	C_9	C_{10}	C_{11}	C_{12}	C_{13}	C_{14}	C_{15}	C_{16}	C_{17}	C_{18}
D	1.6	1.6	1.5	1.4	1.3	1.2	1.1	1.0	0.9	0.9	0.8	0.7	0.6	0.6	0.5	0.4	0.3	0.3	0.2

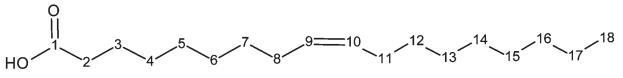

value of 5.1 D (see the Supporting Information for partial charges). Here we focus on results obtained using RESP charges, while results obtained with PRODRG charges are provided in the Supporting Information.[39]

2.2. Molecular Dynamics Simulations. All MD simulations and analyses were carried out with the GROMACS 3.3 and 4.0 packages.[40,41] Two different initial positions were considered for each quercetin derivative: (i) inside the lipid bilayer and (ii) outside the bilayer, i.e., fully solvated compound without any contact with the membrane. A single quercetin derivative was present in each simulation that took at least 100 ns. However, when final locations of the derivative were different starting from both initial locations, the MD simulations were extended (up to 300 ns) to reach location convergence (Table S1 and Figure S1 in the Supporting Information). At this point, the molecule began to fluctuate around this position. Because most of studied molecules were located at the end inside the lipid bilayer/water interface, convergence was reached quicker when starting from the former initial position (at the center of lipid bilayer). MD simulations were performed with different random initial velocities sampled from the Maxwell distribution to enhance sampling and to ensure convergence of the different analyzed metrics (e.g., energy, location, and orientation).

Newton's equations were integrated by the leapfrog algorithm using a 2 fs time step. All bonds were constrained by the LINCS algorithm.[42] Geometries and energies were saved every 0.2 and 0.5 ps, respectively. Periodic boundary conditions were applied. In simulations employing RESP charges, the electrostatic interactions were computed by the particle-mesh Ewald method[43,44] in which real-space Coulomb and Lennard-Jones interactions were cutoff at 1.4 nm. These simulations were carried out at 310 K in the NPT ensemble using the velocity-rescaling thermostat[45] with a coupling constant of 0.1 ps and the anisotropic Parrinello−Rahman barostat[46,47] with coupling constant 0.1 ps and reference pressure at 1 bar. In simulations employing PRODRG charges, the electrostatic interactions were again computed by the particle-mesh Ewald method[43,44] but with Coulomb and short-range Lennard-Jones interaction cutoffs of 0.9 and 1 nm, respectively. In these simulations, temperature and pressure were controlled by Berendsen thermostat[48] and anisotropic Berendsen barostat,[48] respectively. This protocol was successfully applied in our recent study on ibuprofen and 3-hydroxyibuprofen embedded in DOPC lipid bilayer.[49]

2.3. Analysis. The surfaces of the membrane were defined by the layer of P-atoms of the phosphatidylcholine head groups and were oriented parallel to the *xy*-plane. The distance along the *z*-axis of the quercetin derivative relative to the center of lipid bilayer was used as a metric to study its spatial distribution in the membrane. This analysis was performed using both (i) the center of mass of the entire quercetin derivative, which we refer to as distance *d* and (ii) the centers of masses of its various characteristic groups (3-OH, 3′-OH, 4′-OH, 5-OH, 7-OH, the S-atom, the

COOH group and the O-atom at C4, see Figure 1). The orientation of a quercetin derivative was described by the α-angle defined between the z-axis and the vector perpendicular to the plane defined by the C2, C3, and C6 atoms (i.e., A- and C-rings). The A- and C-ring moiety is parallel and perpendicular to the surface of the membrane when α equals 0° (180°) and 90°, respectively.

The number of H-bonds (X—H···Y) was analyzed assuming the presence of a H-bond when (i) the distance between H-bond donor and acceptor d(X−Y) was lower than 3.5 Å and (ii) the angle H−X−Y was lower than 30°. Analysis of the distributions of position, orientation, and number of H-bonds was performed over the last 5 ns of MD simulations, i.e., over the portion of the trajectory deemed to be well equilibrated and sufficiently representative of a real system.

2.4. Potential of Mean Force Calculations. Umbrella sampling[50] calculations were also performed to enable thorough sampling of all quercetin-derivative positions across the full extent of the lipid bilayer, thus overcoming the Boltzmann sampling limits of plain MD simulations and yielding converged free energy (ΔG) profiles (potentials of mean force, PMFs) and associated probability distributions to a high level of statistical certainty. An initial set of sampling windows was prepared by pulling the molecule along the z-axis from the center of bilayer (d = 0 nm) to the wall of the water box (d = 3.5 nm) during a 1 ns simulation. Forty-five geometries from this initial run were then used as initial configurations for sampling windows equally spaced every angstrom along the z-axis. During each MD simulation, an umbrella restraint was applied to motion of the molecule along the z-axis, while motions in the xy-plane were not restrained. The umbrella restraint used a spring constant of 1000 kJ·mol·nm^{-2}, a value that guaranteed sufficient overlap of the histograms of adjacent windows (see Figure 5C). Sampling runs of 25 ns per window were done to obtain convergent simulations as determined by free energy profile convergence and correlation times (correlation times in different umbrella sampling windows were ranging from 100 to 3000 ps). Averaging (and error bar determination) was performed over the last 15 ns to allow a better sampling and more realistic error bars. Due to membrane symmetry, the ΔG profiles were calculated only for half the box using the g_wham[51] implementation of the weighted histogram analysis method. Statistical uncertainties were estimated using the bootstrapping of complete histograms method implemented in g_wham.

3. RESULTS AND DISCUSSION

3.1. Position and Orientation of Quercetin in Membranes. Final geometries of all MD simulations indicate that quercetin systematically incorporates into the lipid bilayer, regardless of its initial location and orientation. The quercetin equilibrated position is between the hydrophobic core and polar surface of lipid bilayer (Figure 2A). When starting in the water phase, quercetin approaches the surface of the lipid bilayer within 20 ns, and then enters the bilayer, where its center of mass position d fluctuates about an average value 1.5 nm with a standard deviation of 0.2 nm (Figure 3A, Figure S1 in the Supporting Information and Table 1). When starting inside the lipid bilayer (d = 0 nm), quercetin relaxes to the same position within around 10 ns. This finding is supported by the ΔG profile (Figure 4) obtained from umbrella sampling simulations, which indicates the presence of a broad free energy well centered at 1.5 nm with 90% of the probability density lying in the range 1.2−2.1 nm. The free energy minimum is around 7.8 ± 0.3 kcal/mol more stable than in the water phase (Figure 4). The penetration is barrierless, with the free energy steadily decreasing from the water phase to the free energy minimum, thus confirming that quercetin readily penetrates lipid bilayers. The energetic cost (14.1 ± 0.7 kcal/mol) to penetrate toward the center of bilayer is, however, significant (see Figure 4).

The fact that the free energy minimum is inside the lipid bilayer but close to the polar head groups of the bilayer surface reflects the amphipathic character of quercetin having both hydrophobic aromatic rings and hydrophilic OH groups (Figure 1). The OH groups interact with the polar heads of lipids by H-bonding; quercetin has an average of three H-bonds with DOPC polar head (Table 2). The five OH groups of quercetin are nearly at the same distance from the center of lipid bilayer (Figure 5A and Table 1), which indicates that the molecule is almost parallel to the surface (Figure 2A). The distribution of the α-angle (between z-axis and the normal of the plane defined by the A- and C-rings) displays a maximum around 30° (Figure S2A in the Supporting Information).

The location of all compounds in the lipid bilayer affects membrane properties, including, e.g., thickness. In the case of quercetin, its incorporation in a membrane induces a deformation of the membrane surface. At the position where the molecule is located, a small cavity of water molecules is formed (P-atoms close to the molecule are 0.2 nm deeper with respect to P-atoms far from the molecule) and thus the thickness of membrane is reduced. This is in very good agreement with the strong alteration of the structural properties of lipid bilayer induced by quercetin.[23] Depending on the incorporation depth, this deformation may favor H-bonds between the polyphenol and the water molecules of this cavity.

In conclusion, quercetin locates below the surface of lipid bilayer. This location of quercetin agrees well with that identified from fluorescence experiments in DPPC (1,2-dipalmitoyl-*sn*-glycero-3-phosphocholine) liposomes and human skin fibroblast cells.[19] In this position and orientation, the free-radical-scavenger active OH groups (3-OH, 4′-OH, and 3′-OH) of quercetin are located around 1.5 ± 0.2 nm from the center of membrane (Table 1). The molecule thus appears as an effective barrier to free radicals flowing across the membrane (e.g., $^{\bullet}$OH free radicals) by scavenging them and inhibiting initiation of lipid peroxidation. MD simulations indicate that quercetin is not the most adapted LOO$^{\bullet}$ radical scavenger, as the active free radical scavenger groups are far from the region where these radicals are formed.[52] This result is in agreement with some experimental data reported that flavonoids do not scavenge these radicals.[53−55]

3.2. Position and Orientation of Quercetin Metabolites in Membranes: Influence of Substitutions. All quercetin metabolites (Figure 1) are globally less active than quercetin as free-radical scavengers and lipid peroxidation inhibitors.[26] At physiological conditions (pH ∼ 7), glucuronide and sulfate conjugates are mostly found in their deprotonated forms (negatively charged). Both protonated and deprotonated forms were studied and differences in their location and orientation are discussed here.

(a). Methylated Metabolites. The presence of the methoxy group does not significantly affect the average position of 3′-*O*-methyl-quercetin in the lipid bilayer compared to quercetin. The average position of the center of mass is stabilized at d = 1.8 ± 0.3 nm (Table 1 and Figure 3B and Figure S1 in the Supporting Information). The 3-OH, 5-OH, and 4-carbonyl groups are pointing

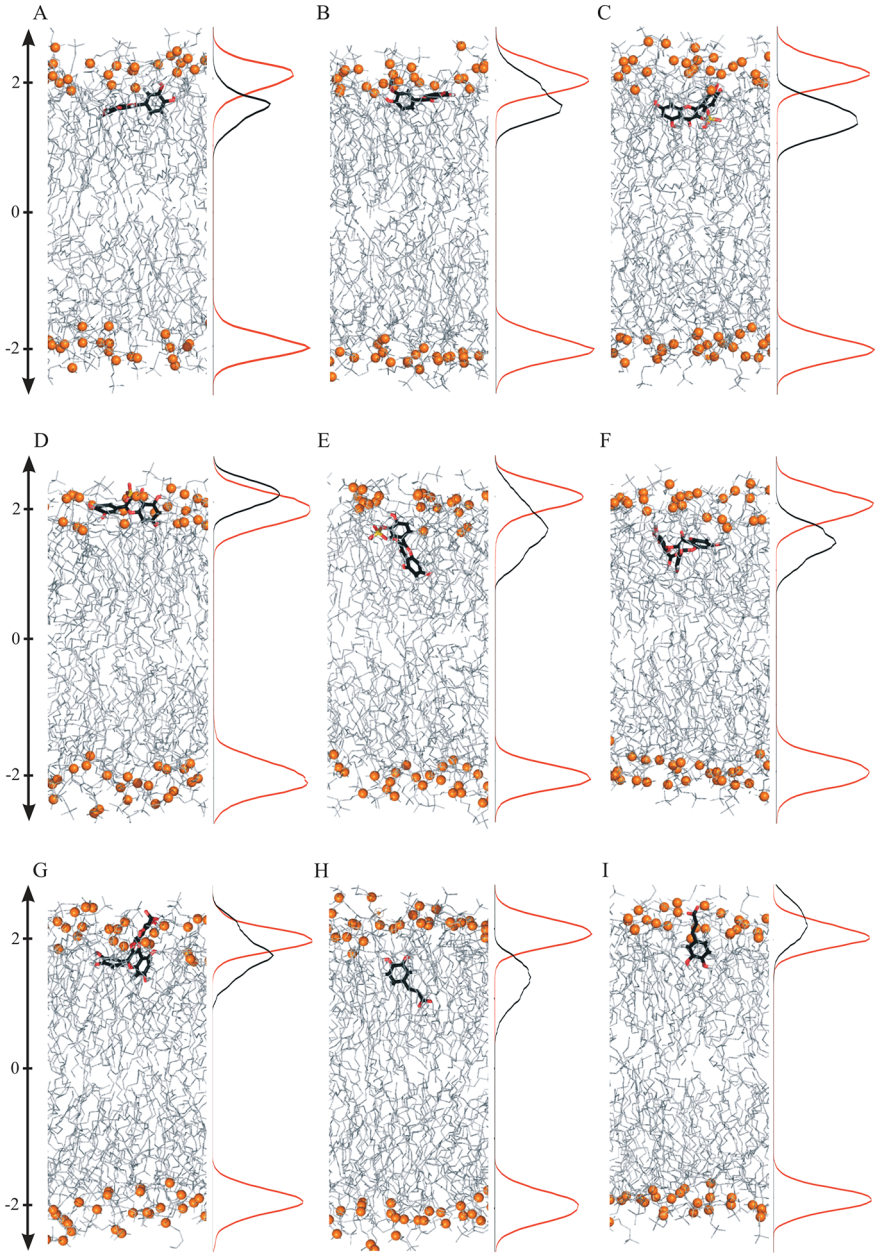

Figure 2. Snapshots of plain MD simulations characteristic to the location of (A) quercetin, (B) 3′-*O*-methylquercetin, (C) protonated form of quercetin-3-*O*-sulfate, (D) deprotonated form of quercetin-3-*O*-sulfate, (E) protonated form of quercetin-3′-*O*-sulfate, (F) protonated form of quercetin-3-*O*-glucuronide, (G) deprotonated form of quercetin-3-*O*-glucuronide, (H) protonated form of caffeic acid, and (I) deprotonated form of caffeic acid. The orange balls and lines describe phosphorus atoms. Each snapshot is chosen to be representative of the average location and orientation of the compound.

toward solvent and the B-ring is clearly immersed in the hydrophobic core (Figure 5B and Table 1). The α-angle distribution exhibits two maxima at 90° and 40° (Figure S2 in the Supporting Information).[56] The former corresponds to perpendicular orientation of the A- and C-ring moiety as regards the surface of lipid bilayer.

The orientation of 3′-*O*-methylquercetin thus differs from that of quercetin. The 3-OH group is nearly at the same distance as P-atoms of the surface of membrane; this position shows that the 3-OH group definitely does not participate in the direct $LOO^{\bullet}$ free-radical scavenging. The B-ring (3′-OCH_3 and 4′-OH groups) is close to the carbonyl and ester groups of DOPC (Table 1). Moreover, in this case, the 3′-OCH_3 group is inactivated and only the 4′-OH group is able to scavenge free radicals. Its activity is decreased due to the absence of the *ortho* OH group (the catechol moiety is replaced by the less active guaiacyl moiety).[57] This is probably the main reason for the reduced lipid peroxidation activity of 3′-*O*-methylquercetin compared to quercetin.

(b). Sulfated Metabolites. The protonated form of sulfate derivatives is marginal in water at physiological conditions and its deprotonated form dominates. The negative charge of the deprotonated sulfate group favors electrostatic and H-bonding interactions with water molecules; i.e., for quercetin-3-*O*-sulfate

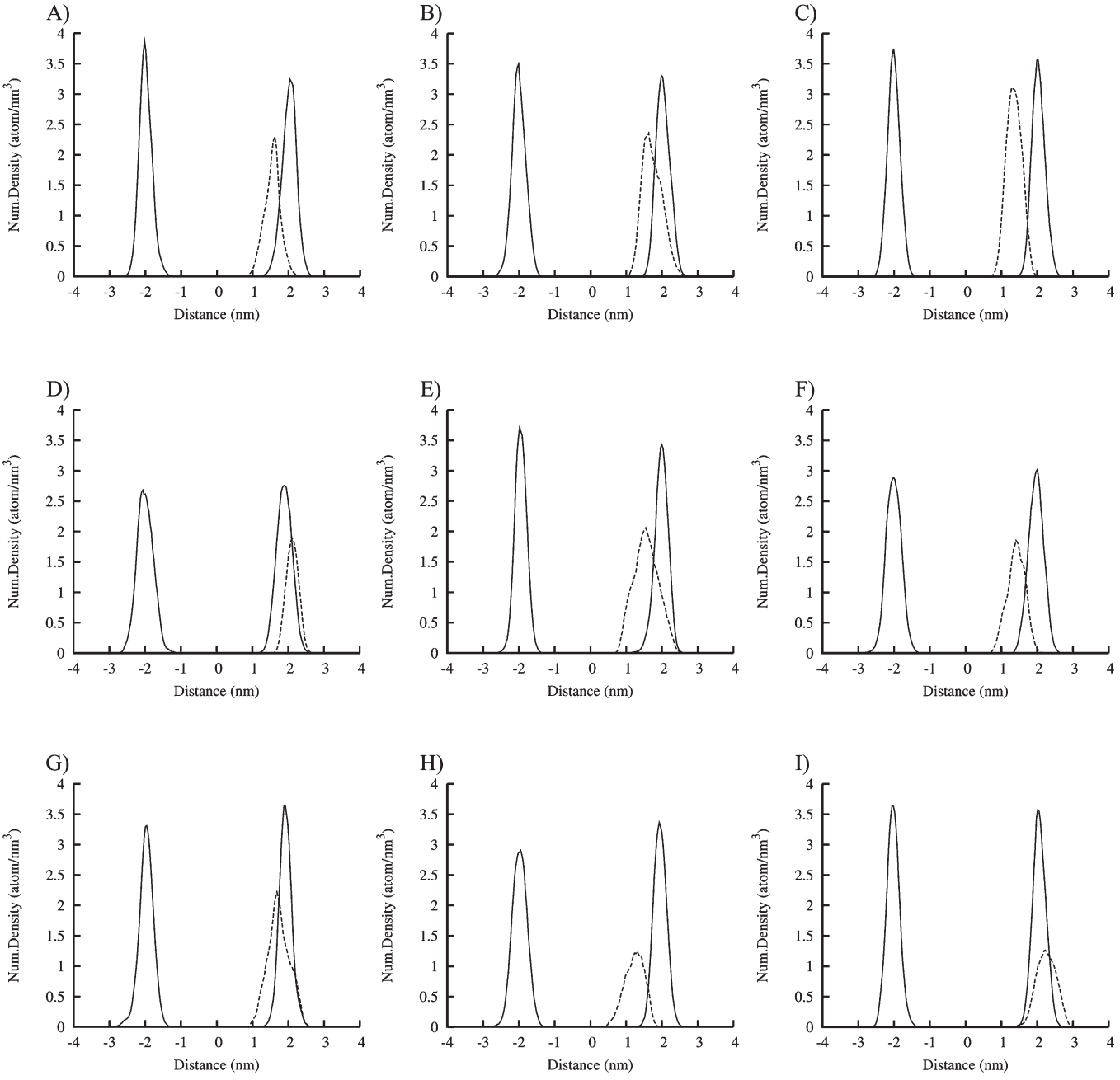

Figure 3. Distribution of the number densities (dashed line) describing the position of (A) quercetin, (B) 3′-*O*-methylquercetin, (C) protonated form of quercetin-3-*O*-sulfate, (D) deprotonated form of quercetin-3-*O*-sulfate, (E) protonated form of quercetin-3′-*O*-sulfate, (F) protonated form of quercetin-3-*O*-glucuronide, (G) deprotonated form of quercetin-3-*O*-glucuronide, (H) protonated form of caffeic acid, and (I) deprotonated form of caffeic acid. The black curves denote the position of phosphorus atoms.

there are 6 ± 3 H-bonds with water (Table 2). This naturally attracts the molecule to the water phase; the position of the center of mass is $d = 2.1 \pm 0.2$ nm (Table 1 and Figure 3D). The sulfate moiety is anchored in the surface of lipid bilayer (Figure 5D). This location induces a bump in the P-atom surface leading to a local increase of the bilayer thickness (P-atoms far from the molecule are 0.3 nm deeper with respect to P-atoms close to the molecule). The main part of the molecule is kept inside the lipid bilayer but most of the OH groups are located at 2.0 ± 0.2 nm. However, the molecule is not parallel to the surface and the α-angle fluctuates around two minima, around 40° and 80° (Figure S2D in the Supporting Information), thus positioning the 7-OH group deeper inside lipid bilayer (1.7 ± 0.1 nm, see Table 1). The B-ring is mainly orientated toward the surface of bilayer close to the P-atoms of the surface (Table 1), which would significantly modify the lipid peroxidation inhibition capacity of this metabolite compared to quercetin. In particular, the type of radicals to be scavenged would be modified. Again, this quercetin metabolite is far from the double bond and definitely cannot scavenge $LOO^{\bullet}$ free radicals and inhibit the propagation step. A similar behavior is observed for quercetin-3′-*O*-sulfate, for which the free-radical-scavenger active 3-OH and 4′-OH groups are located around 2 nm from the center of lipid bilayer (Table 1).

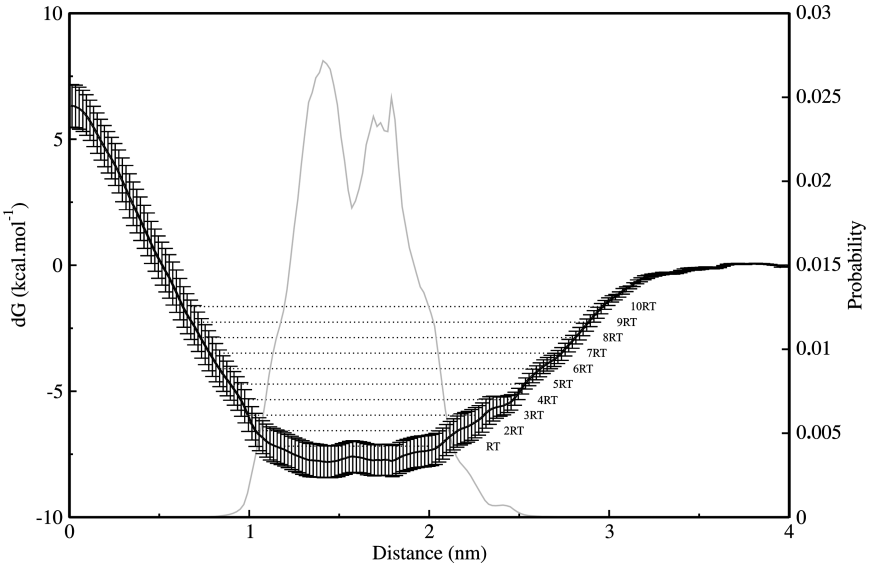

Figure 4. Free energy profile for penetration of quercetin in the lipid bilayer, i.e., from the wall of the water box (d = 3.5 nm) to the center of bilayer (d = 0 nm). *nRT* is drawn as horizontal lines to show the flexibility around the equilibrium location. The double scale corresponds to the probability distribution.

Table 2. Average Number of H-Bonds and Corresponding Standard Deviations between the Solute and Both the DOPC Lipid Bilayer and the Water Molecules

	DOPC molecule		water molecule		total		
	H-bonds	pairs	H-bonds	pairs	H-bonds	pairs	Suma
quercetin	2.9 ± 0.7	2.7 ± 1.9	1.1 ± 1.0	3.1 ± 2.4	4.0 ± 0.9	5.8 ± 3.1	9.8 ± 3.4
3′-*O*-methylquercetin	2.3 ± 0.8	1.7 ± 1.1	2.2 ± 1.5	8.5 ± 5.0	4.5 ± 1.3	10.2 ± 5.1	14.7 ± 5.5
quercetin-3-*O*-sulfate[a]	3.3 ± 0.8	1.8 ± 1.4	1.4 ± 1.0	5.7 ± 2.8	4.7 ± 0.9	7.5 ± 3.2	12.2 ± 3.5
quercetin-3-*O*-sulfate	2.8 ± 0.9	1.4 ± 1.3	6.2 ± 2.6	8.6 ± 4.7	9.0 ± 2.0	10.0 ± 4.0	19.0 ± 5.3
quercetin-3′-*O*-sulfate[a]	2.4 ± 0.7	1.5 ± 1.3	2.3 ± 1.2	6.8 ± 5.0	4.7 ± 0.8	8.4 ± 5.6	13.1 ± 5.8
quercetin-3′-*O*-sulfate	2.0 ± 0.6	1.5 ± 1.2	4.1 ± 1.8	7.1 ± 4.0	6.1 ± 1.7	8.6 ± 3.7	14.7 ± 4.5
quercetin-3-*O*-glucuronide[a]	4.3 ± 0.9	2.3 ± 1.9	4.2 ± 1.0	7.0 ± 2.4	8.5 ± 1.4	9.3 ± 2.5	17.8 ± 2.9
quercetin-3-*O*-glucuronide	4.3 ± 1.3	1.4 ± 1.2	10.8 ± 1.9	14.3 ± 3.8	15.1 ± 2.5	15.7 ± 4.0	30.8 ± 5.3
caffeic acid[a]	2.0 ± 0.0	0.5 ± 0.7	0.5 ± 0.6	1.5 ± 1.7	2.5 ± 0.6	2.0 ± 1.7	4.5 ± 2.1
caffeic acid	0.8 ± 0.6	0.8 ± 1.1	6.6 ± 1.7	5.1 ± 2.7	7.4 ± 1.6	5.9 ± 2.7	13.2 ± 3.4

[a] Protonated forms of derivatives are not present in physiological conditions.

For the protonated forms, the center of mass is stabilized deeper inside the lipid bilayer, d = 1.4 ± 0.2 nm (Table 1 and Figure 3C,E) since the sulfate moiety does not really act as an anchor in this case.

These results demonstrate that the decrease in the antioxidant activity of sulfate metabolites is (i) partly attributed to the loss of free-radical-scavenging capacity (active sites for HAT are blocked by the OSO_3H group at C3 or C3′) and (ii) partly to the change in location and orientation of the molecule in the bilayer (i.e., the molecule active groups are less located at the position where the lipid peroxidation reactions occur).

(c). Glucuronidated Metabolites. As for sulfate metabolites, the protonated form is marginal. At physiological pH (∼7) the sugar moiety is mostly deprotonated (in water phase) due to its low pK_a (e.g., phenolic acid-glucuronide pK_a is 2.9−3.1[58]). When the initial position of the deprotonated form is inside the lipid bilayer (near the center at the beginning of MD simulation) the quercetin moiety locates inside the membrane and half of the glucuronide moiety is outside (Table 1). The molecule is globally at the interface, d = 1.8 ± 0.2 nm (Table 1 and Figure 3G). The 3-OH group being blocked by the glucuronide moiety, the only free-radical-scavenger active moiety (B-ring) is relatively close to the surface (the 3′- and 4′-OH are located at around 1.7 nm from the center of lipid bilayer, see Table 1). However, due to the size of the molecule the B-ring is still inside (Figure 5G). The presence of the deprotonated glucuronide moiety strongly enhances the electrostatic interaction with the polar surface of the bilayer and the number of H-bonds increases, mainly with water molecules (around eleven H-bonds, see Table 2). The negative charge has another crucial effect since it also makes the passage through the polar barrier of membrane difficult. When MD simulation starts from the water phase, the glucuronide moiety and B-ring of the compound stay outside of lipid bilayer.

The protonated form incorporates the lipid bilayer much easily. In this case, for the stabilized location, the distances of

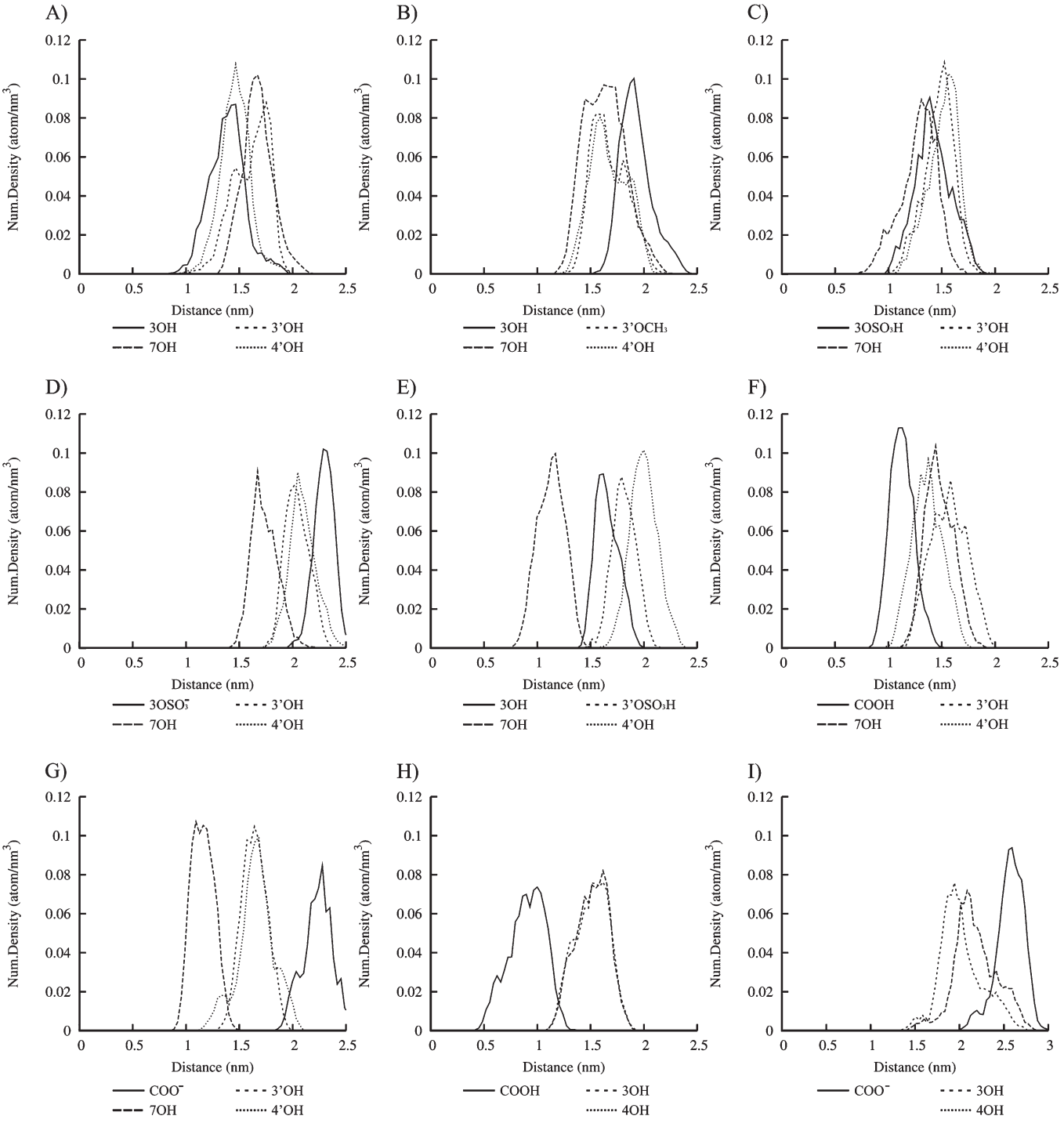

Figure 5. Distribution of the number densities of OH, SO_3H, and COOH groups of (A) quercetin, (B) 3′-*O*-methylquercetin, (C) protonated form of quercetin-3-*O*-sulfate, (D) deprotonated form of quercetin-3-*O*-sulfate, (E) protonated form of quercetin-3′-*O*-sulfate, (F) protonated form of quercetin-3-*O*-glucuronide, (G) deprotonated form of quercetin-3-*O*-glucuronide, (H) protonated form of caffeic acid, and (I) deprotonated form of caffeic acid.

all quercetin OH groups are very similar (Table 1 and Figure 5F), and thus the compound is almost planar to the surface of bilayer (Figure S2 in the Supporting Information). The glucuronide moiety interacts by H-bonding and exhibits around four H-bonds with the polar surface (Table 2).

(d). Position and Orientation of Caffeic Acid. The average location of the center of mass of the protonated form of caffeic acid is relatively deep in the lipid bilayer, $d = 1.2 \pm 0.2$ nm (Table 1, Figures 2H and 3H). The catechol moiety, which is the free-radical-scavenger active group, interacts with the carbonyl group of fatty acids by H-bonding (Table 2). In the protonated form, the OH groups of the catechol moiety may scavenge free-radical initiator coming from outside but also $LOO^{\bullet}$ radicals, depending on lipid unsaturation.

For the deprotonated form of caffeic acid, the negative charge of the carboxyl group enhances electrostatic interaction in particular with water molecules. The center of mass is stabilized at $d = 2.3 \pm 0.2$ nm (Table 1, Figures 2I and 3I) where the molecule has electrostatic and H-bonding interactions (Table 2). The location of the deprotonated caffeic acid disables direct $LOO^{\bullet}$ free-radical scavenging. However, some authors proposed the hypothesis that caffeic acid may not act as a lipid peroxidation inhibitor by itself but as a regenerator agent of other antioxidants incorporated in the membrane (e.g., vitamin E).[59,60]

4. CONCLUSIONS

Quercetin and quercetin metabolites incorporate into the DOPC lipid bilayer, most of these compounds lying just below the surface of bilayer close to the polar head region. Their exact penetration depth and orientation in bilayer are largely determined by their polarity, charges, and H-bonding capacity. The position of quercetin and its metabolites in lipid bilayers depends on (i) the type of substituent, (ii) the substituted OH group, and (iii) charge of the compound. This picture might differ in polyunsaturated and/or oxidized lipid bilayers, for which changes of location/orientation should be systematically evaluated in future.

The partial decrease of lipid peroxidation inhibition observed for 3′-*O*-methylquercetin and quercetin-3-*O*-glucuronide compared to quercetin[26,27] is partially explained by their location and orientation in the lipid bilayer. For both compounds, the substituents pull the compounds very close to the surface in comparison with quercetin. As a consequence, the active OH groups may be less efficient as regenerator of vitamin E and even less efficient at direct $LOO^{\bullet}$ free-radical scavenging. For quercetin-3′-*O*-sulfate, the charged sulfate group pulls the compound out of lipid bilayer, thus explaining its weaker inhibition activity compared to quercetin-3-*O*-glucuronide.

MD simulations demonstrate that flavonoids are concentrated at the lipid bilayer/water interface, just below the membrane surface. Insertion of nonpolar groups increases the penetration depth (methoxy derivatives) while insertion of polar groups decreases the penetration depth (sulfate, glucuronide). Positions and orientations make these compounds potential protector against exogenous attacks (e.g., oxidative stress) being (i) potentially active as lipid peroxidation inhibitors mainly by the scavenging of free radicals initiating lipid oxidation and occasionally those produced during lipid peroxidation propagation[61] or (ii) potential regenerators of antioxidants incorporated in the membrane such as vitamin E.[59,60,62,63]

As flavonoids and their derivatives are preferentially localized in the membrane or on the membrane/water interface, they concentrate in a relatively narrow membrane region. This is of great significance because even if their concentration in food is relatively low, the spatial confinement of flavonoids inside membranes greatly enhances their local concentration in this vital region, thus increasing their importance for in vivo biological activities including oxidative stress defense.

■ ASSOCIATED CONTENT

Ⓢ Supporting Information. Position of the center of mass along the MD simulations for all compounds (molecules described by RESP charges and PRODRG charges), distribution curve of angle defined by bilayer normal and plane defined by atoms C2, C3, and C6 of quercetin (molecules described by RESP charges and PRODRG charges), number densities describing position of compounds in lipid bilayer (compounds described by PRODRG charges), free energy profile for quercetin described by PRODRG charges, average distances of different molecule groups from membrane center, average number of H-bonds (compounds described by PRODRG charges), atomic partial charges and dipole moments of quercetin obtained by different RESP methods, and atomic partial charges of atoms obtained by PRODRG and RESP method. This material is available free of charge via the Internet at http://pubs.acs.org..

■ AUTHOR INFORMATION

Corresponding Author

*E-mail: patrick.trouillas@unilim.fr.

■ ACKNOWLEDGMENT

The authors thank Conseil Régional for the financial support and acknowledge usage of supercomputer Cali (Calcul en Limousin) for computer time. P.K. is also grateful to T. Hendrychová from Palacký University (Olomouc, CZ), who initially helped with Gromacs. Support through GACR grant 303/09/1001. This work was also supported by the Operational Program Research and Development for Innovations—European Regional Development Fund (CZ.1.05/2.1.00/03.0058) and European Social Fund (CZ.1.07/2.3.00/20.0017). Support from the COST Chemistry CMST0804 project is acknowledged. M.W. thanks the EU for financial support through the Marie Curie Research Training Network THREADMILL (MRTN-CT-2006-036040).

■ REFERENCES

(1) Spector, A. A.; Yorek, M. A. *J. Lipid Res.* **1985**, *26*, 1015–1035.
(2) Mouritsen, O. G.; Jorgensen, K. *Pharm. Res.* **1998**, *15*, 1507–1519.
(3) van Meer, G.; Voelker, D. R.; Feigenson, G. W. *Nat. Rev. Mol. Cell Biol.* **2008**, *9*, 112–124.
(4) Niki, E. *Free Radical Biol. Med.* **2009**, *47*, 469–484.
(5) Gutteridge, J. M. *Clin. Chem.* **1995**, *41*, 1819–1828.
(6) Niki, E.; Yoshida, Y.; Saito, Y.; Noguchi, N. *Biochem. Biophys. Res. Commun.* **2005**, *338*, 668–676.
(7) Rikans, L. E.; Hornbrook, K. R. *Biochim. Biophys. Acta, Mol. Basis Dis.* **1997**, *1362*, 116–127.
(8) Logani, M. K.; Davies, R. E. *Lipids* **1980**, *15*, 485–495.
(9) Wang, X.; Quinn, P. J. *Prog. Lipid Res.* **1999**, *38*, 309–336.
(10) Blokhina, O.; Virolainen, E.; Fagerstedt, K. V. *Ann. Bot.* **2003**, *91*, 179–194.
(11) Havsteen, B. H. *Pharmacol. Ther.* **2002**, *96*, 67–202.
(12) Trouillas, P.; Marsal, P.; Siri, D.; Lazzaroni, R.; Duroux, J. *Food Chem.* **2006**, *97*, 679–688.
(13) Saija, A.; Scalese, M.; Lanza, M.; Marzullo, D.; Bonina, F.; Castelli, F. *Free Radical Biol. Med.* **1995**, *19*, 481–486.
(14) Ollila, F.; Halling, K.; Vuorela, P.; Vuorela, H.; Slotte, J. P. *Arch. Biochem. Biophys.* **2002**, *399*, 103–108.
(15) Oteiza, P. I.; Erlejman, A. G.; Verstraeten, S. V.; Keen, C. L.; Fraga, C. G. *Clin. Dev. Immunol.* **2005**, *12*, 19–25.
(16) Tsuchiya, H. *Chem.-Biol. Interact.* **2001**, *134*, 41–54.
(17) Movileanu, L.; Neagoe, I.; Flonta, M. L. *Int. J. Pharm.* **2000**, *205*, 135–146.
(18) Hendrich, A. B.; Malon, R.; Pola, A.; Shirataki, Y.; Motohashi, N.; Michalak, K. *Eur. J. Pharm. Sci.* **2002**, *16*, 201–208.
(19) Pawlikowska-Pawlega, B.; Gruszecki, W.; Misiak, L.; Paduch, R.; Piersiak, T.; Zarzyka, B.; Pawelec, J.; Gawron, A. *Biochim. Biophys. Acta, Biomembr.* **2007**, *1768*, 2195–2204.

(20) Terao, J.; Piskula, M.; Yao, Q. *Arch. Biochem. Biophys.* **1994**, *308*, 278–284.
(21) Arora, A.; Byrem, T. M.; Nair, M. G.; Strasburg, G. M. *Arch. Biochem. Biophys.* **2000**, *373*, 102–109.
(22) Castelli, F.; Uccella, N.; Trombetta, D.; Saija, A. *J. Agric. Food Chem.* **1999**, *47*, 991–995.
(23) Wójtowicz, K.; Pawlikowska-Pawlega, B.; Gawron, A.; Misiak, L. E.; Gruszecki, W. I. *Folia Histochem. Cytobiol.* **1996**, *34*, 49–50.
(24) Pawlikowska-Pawlega, B.; Gruszecki, W. I.; Misiak, L. E.; Gawron, A. *Biochem. Pharmacol.* **2003**, *66*, 605–612.
(25) Rice-Evans, C. A.; Miller, N. J.; Paganga, G. *Free Radical Biol. Med.* **1996**, *20*, 933–956.
(26) Loke, W. M.; Proudfoot, J. M.; Mckinley, A. J.; Needs, P. W.; Kroon, P. A.; Hodgson, J. M.; Croft, K. D. *J. Agr. Food Chem.* **2008**, *56*, 3609–3615.
(27) Loke, W. M.; Proudfoot, J. M.; Stewart, S.; McKinley, A. J.; Needs, P. W.; Kroon, P. A.; Hodgson, J. M.; Croft, K. D. *Biochem. Pharmacol.* **2008**, *75*, 1045–1053.
(28) Morand, C.; Crespy, V.; Manach, C.; Besson, C.; Demigné, C.; Rémésy, C. *Am. J. Physiol.-Reg. I* **1998**, *275*, R212–R219.
(29) Kroon, P. A.; Clifford, M. N.; Crozier, A.; Day, A. J.; Donovan, J. L.; Manach, C.; Williamson, G. *Am. J. Clin. Nutr.* **2004**, *80*, 15–21.
(30) Siu, S. W. I.; Vácha, R.; Jungwirth, P.; Böckmann, R. A. *J. Chem. Phys.* **2008**, *128* (125103), 1–12.
(31) Poger, D.; Mark, A. E. *J. Chem. Theory Comput.* **2010**, *6*, 325–336.
(32) Berendsen, H.; Postma, J.; van Gunsteren, W.; Hermans, J. *Intermolecular Forces*, Pullman, B., Eds.; Reidel Publishing Co.: Dordrecht, The Netherlands, 1981; pp 331−342.
(33) Wang, J.; Cieplak, P.; Kollman, P. *J. Comput. Chem.* **2000**, *21*, 1049–1074.
(34) Schüttelkopf, A. W.; van Aalten, D. M. F. *Acta Crystallogr., Sect. D Biol. Crystallogr.* **2004**, *60*, 1355–1363.
(35) Oostenbrink, C.; Villa, A.; Mark, A. E.; van Gunsteren, W. F. *J. Comput. Chem.* **2004**, *25*, 1656–1676.
(36) Boggara, M. B.; Krishnamoorti, R. *Biophys. J.* **2010**, *98*, 586–595.
(37) Lemkul, J. A.; Allen, W. J.; Bevan, D. R. *J. Chem. Inf. Model.* **2010**, *50*, 2221–2235.
(38) Zgarbová, M.; Otyepka, M.; Šponer, J.; Hobza, P.; Jurečka, P. *Phys. Chem. Chem. Phys.* **2010**, *12*, 10476–10476.
(39) The partial charges are crucial for the balanced description of noncovalent interactions in empirical potentials. Simulations performed with PRODRG charges were shown to lead to wrong partitioning properties.[37] In our case, the final equilibrated position of quercetin with PRODRG charges is shifted into the hydrophobic core of lipid bilayer than in the case of RESP partial charges (cf. 1.2 ± 0.2 nm and 1.7 ± 0.1 nm from the center of the bilayer, respectively). This shift can be attributed to the underestimation of partial charges in the case of PRODRG. A similar shift into the lipid bilayer with PRODRG charges in comparison to RESP charges was observed for 3′-*O*-methylquercetin and quercetin-3-*O*-glucuronide (Table S2 and Figure S3 in the Supporting Information). On the other hand, PRODRG assigns more than 2 times more polar charges on the sulfate group. Consequently, the sulfate group pulls sulfate conjugates toward the polar surface and the final position is shifted toward the water phase in contrast to RESP charges. As can be seen, the choice of partial charges can dramatically influence the penetration depth.
(40) Lindahl, E.; Hess, B.; van der Spoel, D. *J. Mol. Model.* **2001**, *7*, 306–317.
(41) Hess, B.; Kutzner, C.; van der Spoel, D.; Lindahl, E. *J. Chem. Theory Comput.* **2008**, *4*, 435–447.
(42) Hess, B.; Bekker, H.; Berendsen, H.; Fraaije, J. *J. Comput. Chem.* **1997**, *18*, 1463–1472.
(43) Darden, T.; York, D.; Pedersen, L. *J. Chem. Phys.* **1993**, *98*, 10089–10089.
(44) Essmann, U.; Perera, L.; Berkowitz, M.; Darden, T.; Lee, H.; Pedersen, L. *J. Chem. Phys.* **1995**, *103*, 8577–8593.
(45) Bussi, G.; Donadio, D.; Parrinello, M. J. *Chem. Phys.* **2007**, *126* (014101), 1–7.
(46) Nosé, S.; Klein, M. L. *Mol. Phys.* **1983**, *50*, 1055–1076.
(47) Parrinello, M.; Rahman, A. *J. Appl. Phys.* **1981**, *52*, 7182–7190.
(48) Berendsen, H. J. C.; Postma, J. P. M.; van Gunsteren, W. F.; DiNola, A.; Haak, J. R. *J. Chem. Phys.* **1984**, *81*, 3684–3690.
(49) Berka, K.; Hendrychová, T; Anzenbacher, P.; Otyepka, M. *J. Phys. Chem. A* **2011**, *115*, 11248–11255.
(50) Torrie, G. M.; Valleau, J. P. *J. Comput. Phys.* **1977**, *23*, 187–199.
(51) Hub, J. S.; de Groot, B. L.; van der Spoel, D. *J. Chem. Theory Comput.* **2010**, *6*, 3713–3720.
(52) Vitrac, H.; Hauville, C.; Collin, F.; Couturier, M.; Thérond, P.; Delaforge, M.; Rémita, S.; Jore, D.; Gardès-Albert, M. *Free Radical Res.* **2005**, *39*, 519–528.
(53) Goupy, P.; Vulcain, E.; Caris-Veyrat, C.; Dangles, O. *Free Radical Biol. Med.* **2007**, *43*, 933–946.
(54) Roche, M.; Dufour, C.; Mora, N.; Dangles, O. *Org. Biomol. Chem.* **2005**, *3*, 423–423.
(55) Vulcain, E.; Goupy, P.; Caris-Veyrat, C.; Dangles, O. *Free Radical Res.* **2005**, *39*, 547–563.
(56) When the molecules approach the minimal position from the water phase, they are more likely perpendicular to the surface of the membrane. When the molecule approaches its minimal position from the center of the membrane, the α-angle is mostly 40°. The most realistic orientation is more probably the former, at least just after penetration. After a longer stay in the membrane, both locations are possible.
(57) Anouar, E.; Calliste, C. A.; Košinová, P.; Di Meo, F.; Duroux, J. L.; Champavier, Y.; Marakchi, K.; Trouillas, P. *J. Phys. Chem. A* **2009**, *113*, 13881–13891.
(58) Farrell, T.; Poquet, L.; Dionisi, F.; Barron, D.; Williamson, G. *J. Pharm. Biomed.* **2011**, *55*, 1245–1254.
(59) Iglesias, J.; Pazos, M.; Andersen, M. L.; Skibsted, L. H.; Medina, I. *J. Agric. Food Chem.* **2009**, *57*, 675–681.
(60) Laranjinha, J.; Vieira, O.; Madeira, V.; Almeida, L. *Arch. Biochem. Biophys.* **1995**, *323*, 373–381.
(61) Sánchez-Moreno, C.; Larrauri, J.; Saura-Calixto, F. *Food Res. Int.* **1999**, *32*, 407–412.
(62) Zhou, B.; Jia, Z.; Chen, Z.; Yang, L.; Wu, L.; Liu, Z. *J. Chem. Soc. Perkins Trans. 2* **2000**, *4*, 785–791.
(63) Zhou, B.; Wu, L.; Yang, L.; Liu, Z. *Free Radical Biol. Med.* **2005**, *38*, 78–84.